Eur Biophys J (1997) 26: 319–326

ARTICLE

Valeri P. Shcherbakov · Michael Winklhofer
Marianne Hanzlik · Nikolai Petersen

Elastic stability of chains of magnetosomes in magnetotactic bacteria

Received: 10 February 1997 / Accepted: 9 April 1997

Abstract Electron micrographs of magnetotactic bacteria reveal that chains of magnetosomes are often bent. This is surprising inasmuch as straight chains are actually the most favourable arrangement for magnetonavigation achieving the maximum value of the bacterial net magnetic moment. In order to answer the question of what causes the chains to bend, we calculated the stability limit of straight magnetosome chains by taking into account elastic and magnetic forces. For several scenarios, the threshold values of external forces leading to elastic instability were computed. From our calculations and observations on freeze-dried cells, we conclude that, under normal conditions, magnetosome chains are straight or only slightly bent, whereas shrinkage during preparation may cause severe artifacts such as kinks or zig-zag structures in the chains.

Key words Bacteria · Magnetotaxis · TEM microscopy · Lipid bilayers

1 Introduction

Magnetotactic bacteria, first observed in 1975 (Blakemore 1975), are regarded as the best understood organism using the Earth's magnetic field for orientation. Their "organ" of magnetonavigation is evident: A chain of intracellular, ferromagnetic single-domain (SD) particles constituting a biomagnetic compass-needle with a magnetic moment m sufficiently large to enable orientation of the bacterium in the geomagnetic field $B_e(r)$ (Frankel and Blakemore 1980), i. e. its magnetic alignment energy $m \cdot B_e$ is one order of magnitude greater than the thermal energy $k_B T$. From a magnetic point of view, a 0.6-μm-long single-domain magnetite bar with cross-section 0.1-μm would easily serve for the purpose of magnetotaxis, yielding a 90% alignment in a magnetic field of 0.5 Gauß ($m \cdot B_e = 16\ k_B T$). Taking into consideration that bacteria reproduce by cell division, however, one automatically has to draw the conclusion that the bacterial organ of magnetoreception in mature cells needs to be composed of at least two such subunits so as to guarantee a successful division process (Kirschvink 1982). Nonetheless, the question arises of why bacteria do pos-

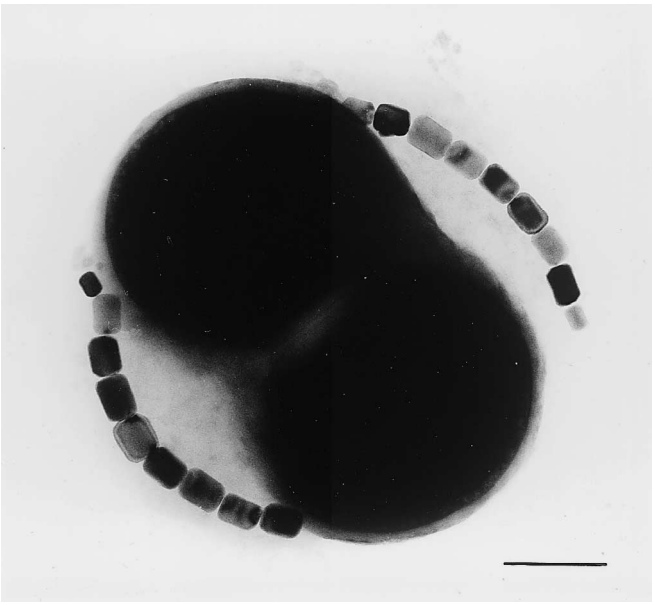

Fig. 1 TEM micrograph of an air-dried magnetic coccus with two chains of magnetosomes. The chains, which lie at opposite sides within the cell body, are bent and thereby fit the shape given by the bacterial cell body. The *scale bar* is 0.2 micron

V. P. Shcherbakov
Geophysical Observatory "Borok", Borok Yaroslavskaja oblast, Russia, 151742
(e-mail: valera@geophys.yaroslavl.su)

M. Winklhofer (✉) · M. Hanzlik · N. Petersen
Institut für Allgemeine und Angewandte Geophysik, Ludwig-Maximilians-Universität, Theresienstrasse 41, D-80333 München, Germany
(Fax: 0049-89-2394 4205;
e-mail: michael@alice.geophysik.uni-muenchen.de)

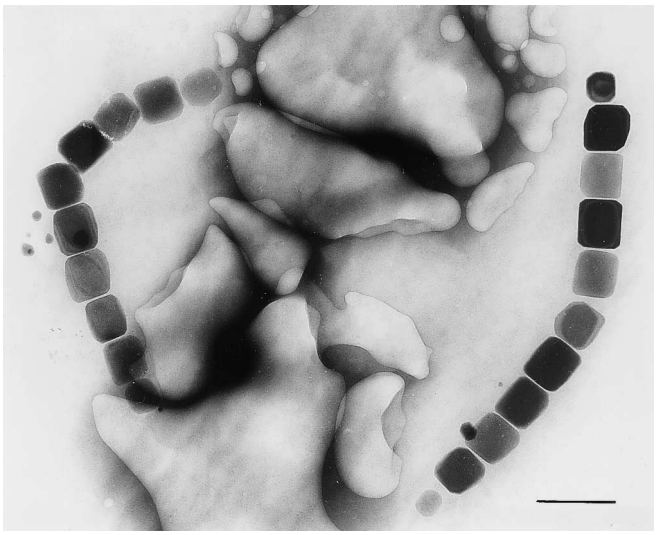

Fig. 2 TEM micrograph of an air-dried magnetic coccus with two chains of magnetosomes with kink. The *scale bar* represents 0.2 micron

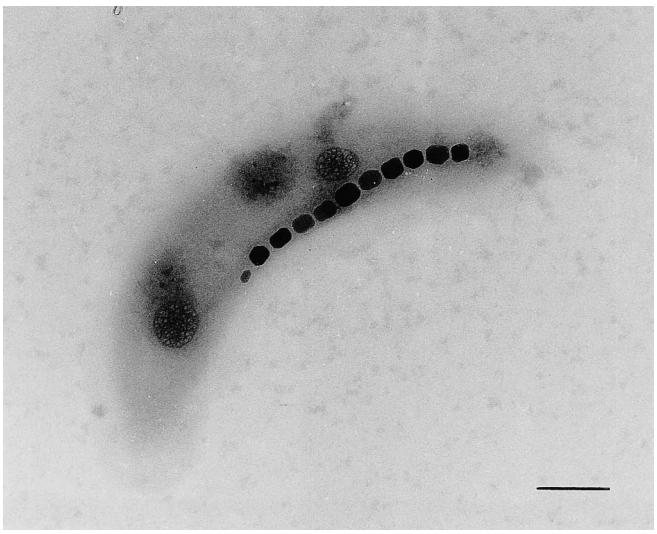

Fig. 3 TEM micrograph of a chain of magnetosomes in an air-dried magnetic spirillum. It can be seen that two neighbouring magnetosomes are separated by a small gap indicating that there is some substance in between which prevents the single-domain particles from sticking together directly. The *scale bar* is 0.2 μm

sess such a device which is far too complex to merely operate as a permanent magnetic dipole. Even if the answer is not known yet, a consequence of this building plan, which allows for flexibility, is that magnetosome chains are often bent (Fig. 1), in certain cases even to such an extent that they form a kink (Fig. 2).

A first analysis of the stability of magnetosome chains has been given by von Dobeneck et al. (1987) using the dipole approximation to describe the magnetic interactions between magnetosomes. In this paper we take into account magnetic as well as elastic forces to calculate threshold values leading to elastic instability for different types of external forces acting on the chain.

2 The model

Our modelling is based on two results obtained from numerous TEM-studies on magnetotactic bacteria:

- Magnetosomes made of magnetite fall into the stable single-domain particle size range, which was first calculated by Butler and Banerjee (1975) and has been confirmed by means of three-dimensional micromagnetic modelling (Fabian et al. 1996).
- Neighbouring magnetosomes of a chain are separated by a small gap filled with some organic material which prevents the magnetically attracting particles from sticking together directly. Gorby et al. (1988) could show for *Magnetospirillum magnetotacticum* (formerly *Aquaspirillum magnetotacticum*) that each magnetosome is enclosed by a lipid bilayer membrane of thickness $h = 6$ nm. The gap-width q in magnetotactic spirilli, however, is often more than $2h$ (Fig. 3), indicating that there is another organic substance (e. g. a protein) in the gap. In other types of bacteria like cocci or vibrios such membranes surrounding the magnetosomes have not been detected yet; but neighbouring magnetosomes in chains of these types of bacteria also lie a distinct distance apart from each other.

2.1 Internal forces in the straight chain

Internal forces in linear chains are a consequence of the strong magnetostatic interactions between neighbouring magnetosomes. There are essentially two contributions to the total energy:

2.1.1 Magnetostatic energy W_{ms}

In case the gap width q is small compared to the diameter a of a magnetosome (Fig. 4 a), the magnetostatic energy W_{ms} between the neighbouring surfaces of two adjacent magnetosomes can be approximated as the magnetostatic self-energy of a thin disc uniformly magnetized along its short axis:

$$W_{ms} = N M_s^2 a^2 q/2 = 2\pi M_s^2 a^2 q \,, \tag{1}$$

where N is the demagnetization factor (here $N = 4\pi$) and M_s the saturation magnetization of the material the magnetosomes are made of. The compressive stress in the gap due to magnetostatic attraction, σ, is then obtained by differentiating W_{ms} with respect to q:

$$\sigma = \frac{1}{a^2}\frac{\partial W_{ms}}{\partial q} = 2\pi M_s^2 \,. \tag{2}$$

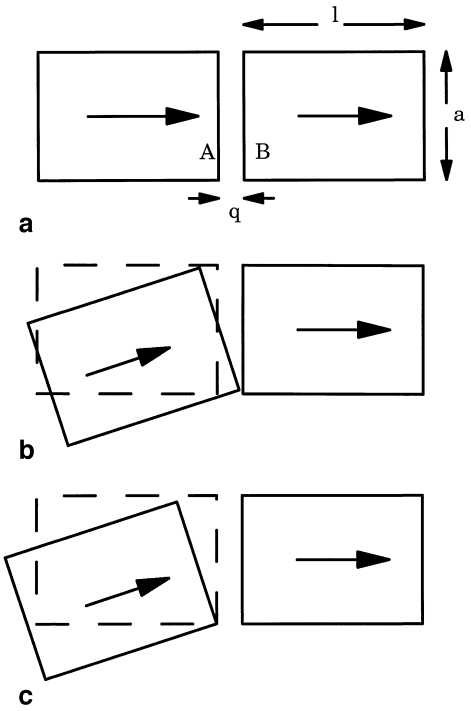

Fig. 4 a–c Three possible arrangements of the neighbouring surfaces A and B of two adjacent magnetosomes as modelled here. Arrows within the particles indicate the direction of magnetization. **a** Parallel configuration as occurring in straight chains. a and l denote the edge-length and the length of each magnetosome, q is the gap-width. **b** Surface A symmetrically tilt with respect to surface B. Since the mean distance between the two surfaces is independent of the tilting angle, inclining the surface by an angle θ in the CW direction is energetically equivalent to the case when the same surface is inclined by θ in the CCW direction. The magnetostatic attraction force between the particles increases as a function of θ. **c** Surface A asymmetrically tilt with respect to surface B. Now the mean distance between the surfaces increases when θ increases, and therefore the magnetostatic attraction between the particles decreases. Note that in **c** the theoretical value of θ can range from $-\sin^{-1}(q/a)$ to π, whereas in **b** is restricted to the intervall $[-\sin^{-1}(2q/a), \sin^{-1}(2q/a)]$

Mostly, magnetosomes consist of magnetite ($M_s = 480$ Gauß) and thus a typical value for the pressure acting on the gap filling amounts of 1.5 bar.

2.1.2 Elastic energy W_{el}

In order to estimate to what extent the organic material is compressed due to magnetostatic attraction forces, knowledge of its elastic properties is required. Although we lack the precise value of its modulus of elasticity E, we can give a lower limit from the following consideration: Employing the usual linear stress-strain relation, $\sigma = Eu$ the elastic and the "magnetic" properties of the gap are related by

$$2\pi M_s^2/E = u_{eq}\,, \tag{3}$$

where u_{eq} is the deformation of equilibrium, which in the following is expressed by the dimensionless parameter J and by definition is less than unity:

$$J := u_{eq} < 1\,. \tag{4}$$

Thus, the value of E has to amount to at least 1.5 bar in order that the gap filling will not get squashed. Before we continue to analyze the stability of linear chains, it seems reasonable to compare this minimum value E^{min} with values characteristic of biological model membranes. The bending rigidity k_C of lipid bilayer membranes (thickness of one layer ~4 nm, Mutz and Helfrich 1990) typically ranges from 0.15×10^{-19} J to 4.15×10^{-19} J (Duwe et al. 1990). The bending rigidity k_C of an isotropic thin elastic plate of thickness h is related to the modulus of elasticity E and Poisson ratio ν by (e. g. Landau and Lifshitz 1970)

$$k_C = \frac{E h^3}{12(1-\nu^2)}\,, \tag{5}$$

and one obtains $E^{exp} = 5 \ldots 200$ bar, which is in fairly good agreement with the minimum value of E^{min} estimated here. Possible large deformations are therefore not primarly due to the magnetic pressure acting between neighbouring particles of a chain, but are the consequence of the anomalously low rigidity of the organic material in between.

2.2 Bending of the chain

In the previous section we have considered a straight chain of magnetosomes compressed by the mutual magnetostatic attraction of its magnetosomes. In the following, the energy of this configuration is compared to that of a chain with one part inclined to the other part by a small angle θ (see Fig. 4 b). In this case, the magnetostatic interaction between the two charged surfaces A and B is not only a function of the distance q between them, but also depends on the tilting angle θ, and we obtain two further contributions to the energy:

2.2.1 Bending energy

In addition to the elastic energy stored in the compressed gap filling, bending elastic energy is necessary to stretch the filling in the part above its neutral line (Fig. 5) and to compress it in the part below. If deformations are small, the additional strain $u - u_{eq}$ related to this bending is proportional to the x-coordinate

$$u_b = u - u_{eq} = ((R+x)\,\theta - R\,\theta)/q = x/R\,, \tag{6}$$

where $R = q/\theta$ is the radius of curvature of the neutral line. The bending energy is then obtained by integrating over a cross section of the elastic material:

$$W_b = \frac{1}{2} E\,a\,q \int_{-a/2}^{+a/2} \left(\frac{x}{R}\right)^2 \mathrm{d}x = \frac{E\,I\,q}{2\,R^2} = \frac{E\,I\,\theta^2}{2\,q}\,. \tag{7}$$

With no loss of generality, the cross-section can be approximated by a square of edge length a leading to $I = a^4/12$ for its moment of inertia.

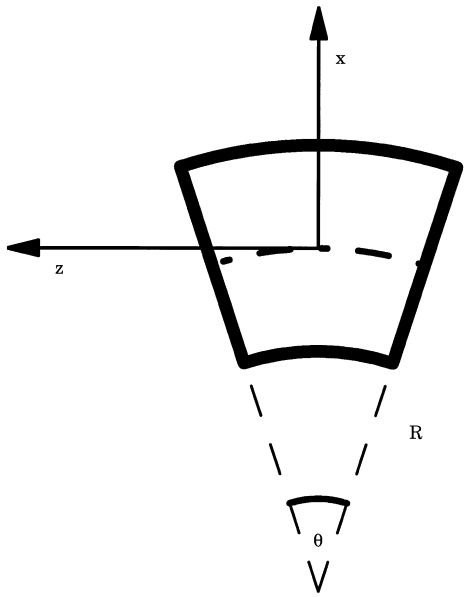

Fig. 5 Bending of the elastic material (long section) in the gap between two magnetosomes which are tilt to each other by a small angle θ (here exaggerated). The neutral line, the length of which remains constant during bending, is represented by the dash-dotted line. Below this line, the material is compressed while it is stretched in the upper part. R denotes the radius of curvature of the neutral line after bending. The strain required for bending is proportional to the x-coordinate (Eq. [6])

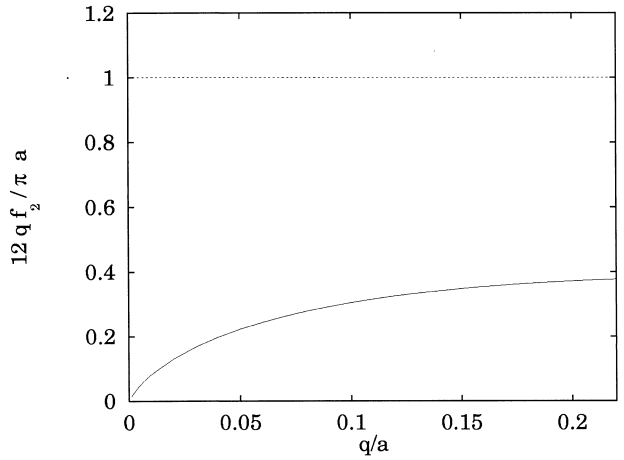

Fig. 6 Stability diagram of the straight chain in absence of external forces. The *solid line* represents the right-hand side of Eq. (10) ($12\,q\,f_2/\pi a$) as a function of the scaled gap width, q/a, the *dashed horizontal line* represents the lower limit of $1/J$, which by definition is greater than unity (Eq. [4])

2.2.2 Magnetostatic energy

As long as $q \ll a$, the condition $\theta \ll 1$ is fulfilled and the magnetostatic energy (Eq. (1)) may be expanded for two surfaces which are slightly inclined to each other:

$$W_{\mathrm{ms}}(q, \theta) = W_{\mathrm{ms}}(q, 0) + F_2(q, 0)\,\theta^2/2! + \ldots . \tag{8}$$

Because of the symmetry of the problem (Fig. 4b), the linear term is zero at $\theta = 0$. The second derivative $F_2(q, \theta) = \partial^2 W_{\mathrm{ms}}(q, \theta)/\partial\theta^2$ is expressed in the same way as $W_{\mathrm{ms}}(q, 0)$, i. e.

$$F_2(q, \theta) = -2 M_s^2 a^3 f_2(q, \theta) .$$

$f_2(q, \theta)$ was obtained by numerical integration of the Rhodes-and-Rowlands formula modified with respect to oblique surfaces (see Eq. (33) – Eq. (35) in the Appendix) and ranges from 2 to 0.5 for ($q/a = 0.01 \ldots 0.2$). The negative sign of the function $F_2(q, \theta)$ indicates that the magnetostatic energy is lowered by tilting because the mean inverse distance between the chains increases. This means that the magnetostatic energy favours bending of the magnetosome chains, whereas the elasticity of the organic material ensures their mechanical stability.

Altogether, we have for those parts of the energy depending on θ:

$$W_{\mathrm{tilt}}(q, \theta) = [E\,I/q - 2 M_s^2 a^3 f_2(q, 0)]\,\theta^2/2 . \tag{9}$$

To achieve instability, the release in magnetostatic energy has to exceed the energy required for bending. This condition leads to the relation

$$1/J < 12\,q\,f_2/\pi a . \tag{10}$$

The stability diagram (Fig. 6) shows that the right-hand side of Eq. (10) is less than unity for gap widths of interest ($q/a = 0.01 \ldots 0.2$), while the left-hand side of Eq. (10) is always greater than unity by definition (see Eq. (4)). Thus, Eq. (10) cannot be fulfilled, which indicates that a linear chain of magnetosomes is an elastically stable arrangement when solely internal contributions to magnetostatic and elastic forces are considered.

From Eq. (9) it can be seen that magnetostatic interactions lead to a reduction of the total energy. The elastic modulus therefore is renormalized as follows:

$$E_{\mathrm{m}} = E\left(1 - \frac{J\,q\,a^3\,f_2}{\pi\,I}\right) = E\left(1 - \frac{12\,J\,q\,f_2}{\pi\,a}\right). \tag{11}$$

3 External force *T*

From the consideration presented above it is obvious that the chain can be regarded as a long rod with interacting alternating elastic (organic substance) and non-elastic (magnetite particles) elements. It is a well-known phenomenon that an elastic rod is subject to instability if an external compressive force T exceeds a critical value F_{crit} (e.g. Timoshenko and Gere 1961). The physical reason for the onset of elastic instability in a compressed straight rod is that bending of it leads to a partial release of the elastic energy which was previously required to compress the rod.

In the following, we analyze the possibilities for onset of elastic instability in a chain of magnetosomes. For this purpose, it is sufficient to consider solely the elastic energy as it implicitly includes the magnetostatic energy (Eq. 11).

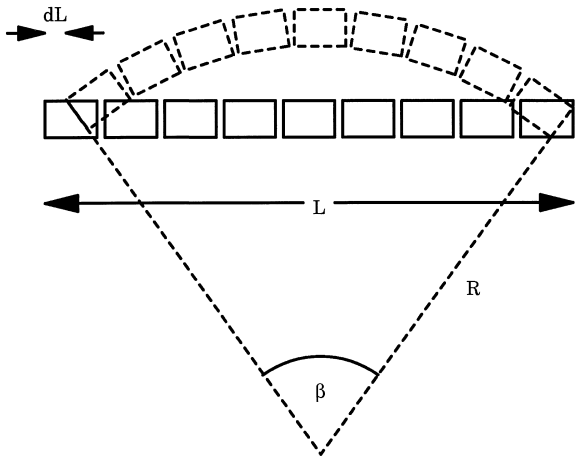

Fig. 7 Sketch of a bent chain of n magnetosomes as modelled here. R is the radius of curvature after bending, $\beta = n\theta$ is the bending angle of the whole chain. L denotes the length of the chain before deformation, $L-\Delta L$ is the length due to compression by an axial force T

3.1 Compressive forces: arc mode

Let α_i be the tilting angle of the i-th chain link (magnetosome). Then, the bending angle between the i-th and $(i+1)$-th link is $\theta_i = \alpha_{i+1} - \alpha_i$. For a rough estimation of F_{crit}, we first assume that all $\theta_i = \theta$ such that $\beta = n\theta$ is the bending angle for the whole chain, which now has the shape of an arc (Fig. 7).

Let $L = n(l+q)$ be the length of the compressed straight rod, where $l > a$ is the length of a magnetosome. In the direction of the axial compressive force T, the rod bent by an angle β is shorter than the straight rod by an amount

$$\Delta L = L - 2R\sin\left(\frac{\beta}{2}\right) = L\left(1 - \sin\left(\frac{\beta}{2}\right)\Big/\left(\frac{\beta}{2}\right)\right) \approx L\beta^2/24\,, \tag{12}$$

where β is assumed to be small such that $\sin(\beta/2)$ may be expanded to the third order and $R = L/\beta$ is the radius of curvature of the neutral line. The work done by an arbitrary force T along the distance ΔL is given by

$$T\,\Delta L = T\,L\,\beta^2/24\,, \tag{13}$$

This gain of elastic strain energy, however, is related to elastic energy required for bending. Summing up the W_{tilt} from Eq. (9), we obtain the total energy of the bent rod as

$$W_{\mathrm{tot}}(q,\beta) = \left[\frac{E_{\mathrm{m}}\,I}{2nq} - \frac{n(l+q)T}{24}\right]\beta^2\,, \tag{14}$$

where only the terms depending on θ are taken into account.

It is useful to express T by means of a dimensionless force,

$$t = 2T\,q(l+q)/E_{\mathrm{m}}I\,, \tag{15}$$

which is related to the relative pressure $\tau = \sigma/E_{\mathrm{m}}$ by

$$t = \tau\,24\,q(l+q)/a^2\,. \tag{16}$$

Equation (14) can now be written as

$$W_{\mathrm{tot}}(q,\beta) = \frac{E_{\mathrm{m}}\,I}{2nq}\left(1 - \frac{n^2 t}{24}\right)\beta^2\,. \tag{17}$$

Since any physically reasonable pressure must satisfy the condition $\sigma/E_{\mathrm{m}} < 1$, the instability condition becomes

$$t > t_{\mathrm{crit}} = 24/n^2\,. \tag{18}$$

If the external, nonmagnetic force exceeds this limit or the chain becomes too long to withstand the external load, the chain will form a smooth arc.

It is also of interest to estimate the critical external pressure using the relation $\sigma_T = T/a^2$ together with Eqs. (16) and (18):

$$\sigma_T^{\mathrm{arc}} = E_{\mathrm{m}}\,\frac{a^2}{2q(l+q)n^2}\,. \tag{19}$$

Under the assumption that $a \approx (l+q)/2$ and $q/a \approx 0.1$, Eq. (19) simplifies to

$$\sigma_T^{\mathrm{arc}} \approx 3E_{\mathrm{m}}/n^2\,. \tag{20}$$

This is an important result: The longer the chain the more easily it can be bent – a fact often to be seen in TEM-micrographs.

In a more general case, the work done by the force T along the distance ΔL is given by

$$T(l+q)\sum_{i=1}^{n}\cos(\alpha_i)\,. \tag{21}$$

Hence, the total energy W_{tot} is given by the following expression:

$$W_{\mathrm{tot}}(q,\alpha_i) = \frac{E_{\mathrm{m}}\,I}{2q}\left[\sum_{i=1}^{n}(\alpha_{i+1}-\alpha_i)^2 - t\sum_{i=1}^{n}\cos(\alpha_i)\right]. \tag{22}$$

This equation can be considered as the discrete analogue of the energy relation for an elastic rod bent in a plane under the influence of a concentrated force (Timoshenko and Gere 1961).

A numerical analysis was carried out to determine t_{min}, the threshold value of t leading to instability. The resulting curve (Fig. 8) excellently fits the formula obtained above (Eq. (18)).

3.2 Compressive forces: kink mode

The consideration presented above is only valid if deflections of the magnetosome chain from the straight line are small: indeed, owing to obvious geometrical restrictions, the bending angles can hardly exceed a critical value θ_0 of order $q/a \approx 0.1$. After this value is achieved, bending can continue in another way by "fixing" the closest end points of the neighbouring surfaces on a distance q and moving away the opposite ones (see Fig. 4c). It is interesting to

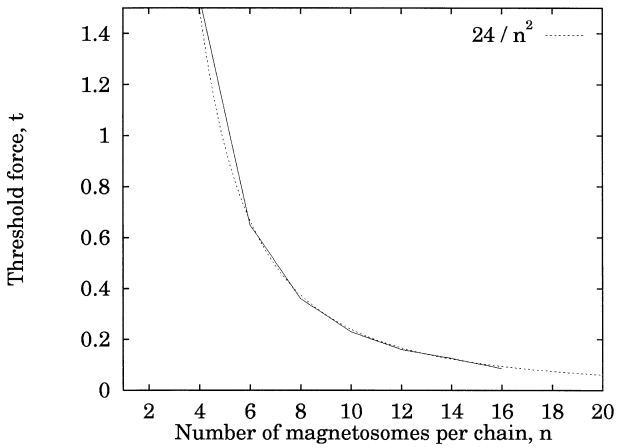

Fig. 8 Numerically determined threshold force $t = t_{\min}$ (*solid line*) required to yield elastic instability of the magnetosome chain as a function of the number of particles *n*. The *dotted line* represents a $1/n^2$ fit (factor 24.01), which is in excellent agreement with the formula obtained in Eq. (18)

note that, for such a process, the roles of the magnetic and the elastic energy completely reverse: the elastic energy decreases while the magnetostatic energy of the arrangement increases and therefore the stabilizing force is provided by the magnetostatic interaction.

Since the gaps widen due to relatively large bending angles, it seems reasonable to neglect the elastic energy in the first approximation. We will proceed with the magnetostatic energy alone and expand it into a Taylor-series:

$$W_{\mathrm{ms}}(q,\theta) = 2M_{\mathrm{s}}^2 a^3 (\text{const.} + f_1(q,0)\,\theta - f_2(q,0)\,\theta^2/2 \ \ldots) \,. \tag{23}$$

Numerical calculations showed that for $q/a = (0.01 \ldots 0.2)$ the values of f_1 range from 1.5 to 0.8 ($f_2 = 6 \ldots 1.5$). Due to the asymmetric arrangement, the first derivative f_1 is no longer zero, which means that the magnetic forces become decisive in the interplay with the external and elastic forces. The total energy of the bent chain is given by

$$W_{\mathrm{tot}}(q,\alpha_i) = -T(l+q)\sum_{i=1}^{n}\{\cos(\alpha_i) + 2\pi M_{\mathrm{s}}^2 a^3 \cdot [f_1(q,0)\,|\alpha_{i+1} - \alpha_i| + f_2(q,0)\,(\alpha_{i+1} - \alpha_i)^2/2]\} \,. \tag{24}$$

As a first assumption, we may neglect the θ_i^2 terms and suppose that bending happens monotonically, that is, $\alpha_i > \alpha_{i-1}$. Thus,

$$W_{\mathrm{tot}}(q,\alpha_i) = 2\pi M_{\mathrm{s}}^2 a^3 f_1(q,0)(\alpha_n - \alpha_1) - T(l+q)\sum_{i=1}^{n}\cos(\alpha_i) \,. \tag{25}$$

Consider the bent chain formed during the first stage of instability and let us again assume that all $\theta_i = \theta$, i.e. the chain forms an arc. By putting $-T(l+q)\sum_{i=1}^{n}\cos(\alpha_i) = \text{const} - T(l+q)\,n^3\theta^2/24$ (see Eq. (13)), we obtain

$$W_{\mathrm{tot}}(q,\theta) = 2\pi M_{\mathrm{s}}^2 a^3 f_1 n\,\theta - T(l+q)\,n^3\theta^2/24 \,. \tag{26}$$

W_{tot} has tendency to increase θ if

$$\frac{\sigma_T}{2\pi M_{\mathrm{s}}^2} > \frac{12\,a\,f_1}{n^2(l+q)\theta} \,. \tag{27}$$

Hence the critical pressure to cause instability is

$$\sigma_{\mathrm{crit}} = E\,\frac{12\,J\,a\,f_1}{(l+q)n^2}\,\theta \,. \tag{28}$$

In particular, it can be seen that the straight chain ($\theta = 0$) is stable with respect to a pure axial compressive force σ_{crit}.

Comparing the value of σ_{crit} with the corresponding value of the Eq. (19) and accepting that $\theta \approx \theta_0 \approx q/2a$ and $a \approx (l+q)/2$, we find that $\sigma_{\mathrm{crit}}/\sigma_T^{\mathrm{arc}} \approx 12\,J$. This is a physically obvious result, for if the modulus of elasticity is large (i.e., $J \ll 1$), a strong external force is required for the onset of the first step of instability and the now comparatively weak magnetic attraction forces cannot stop a further bending such that the chain will collapse as shown in Fig. 9. In contrast, if the critical pressure required to initialize bending is not very large, (i.e., $J \geq 0.1$), then only slightly bent configurations are observed (Fig. 1).

To show how a kink develops, we assume that i) the whole chain is compressed under the action of an external force and ii) the two outermost magnetosomes of a chain are fixed such that the total length of the chain is reduced to $L_1 < L$. Then, the chain has to be bent somehow so as to fulfill this geometrical constraint. In a first approximation, the magnetostatic energy W_{ms} is proportional to $(\alpha_n - \alpha_1)$ (Eq. (25)), and the energetically most favourable configuration is that with a minimum angle difference between the two extreme magnetosomes. It seems obvious that such a configuration is a single and sharp kink in the middle of the chain, which can often be seen in air-dried magnetotactic bacteria (Fig. 2). To prove this supposition, we numerically minimized the energy with respect to the constrained length. We found that the configuration of magnetosomes with a sharp kink in its middle always contains the minimal magnetic energy compared to other configurations. Next we abandoned the linear approximation of $W_{\mathrm{ms}}(\alpha)$ and carried out numerical minimizations using the exact expressions for the magnetostatic interaction between two charged surfaces which are inclined to each other. It turned out again that the kink-mode yields the minimum energy. From the physical point of view this result is quite obvious because the magnetic attraction between the neighbouring surfaces of two adjacent magnetosomes decreases with an increase of the tilting angle, as was pointed out above. Thus, the total energy always is minimal if a chain forms a single, distinct "kink" instead of a number of smaller kinks, as would be the case in the arc-mode.

3.3 External lateral load

Let T_i be a lateral force acting on the *i*-th link (magnetosome) of a chain. If the link moves along a distance Δy in the direction of the force, the associated gain in energy is

$T_i \Delta y$. In the following we are interested in the case that the ends of the chain are supported by the outer membrane and a displacement of the magnetosomes is achieved by bending of the whole chain, i. e.

$$\Delta y = (l+q) \sum_{j=1}^{i} \sin(\alpha_j) . \tag{29}$$

Assuming that all $T_i = T$, the total energy can be expressed as

$$W_{\text{tot}}(q, \alpha_i) = \frac{E_{\text{m}} I}{2q} \sum_{i=1}^{n} \left[(\alpha_{i+1} - \alpha_i)^2 - t \sum_{j=1}^{i} \sin(\alpha_j) \right]. \tag{30}$$

A case of particular interest is when the source of the external force is due to the mutual repulsion of two parallel magnetosome chains. For a rough estimation of the dimensionless force t acting on a chain, we consider the magnetic field H generated by the other chain as that of a dipole with dipole moment $M = M_{\text{s}} a^2 n l$. Then $H \approx M/r^3$, where $r = s a$ is the distance between the chains. As the magnetic moment of a single magnetosome is $M = M_{\text{s}} a^2 l$, the force

$$T = (m \cdot \nabla) H \sim 3 M_s^2 n l^2 / s^4 \tag{31}$$

and

$$t \sim \frac{6 M_s^2 n l^2 q(l+q)}{E_{\text{m}} I s^4} = \frac{36 J n l^2 q(l+q)}{\pi a^4 s^4} \sim 10^{-4} \tag{32}$$

which is obviously too small to cause any noticeable bending.

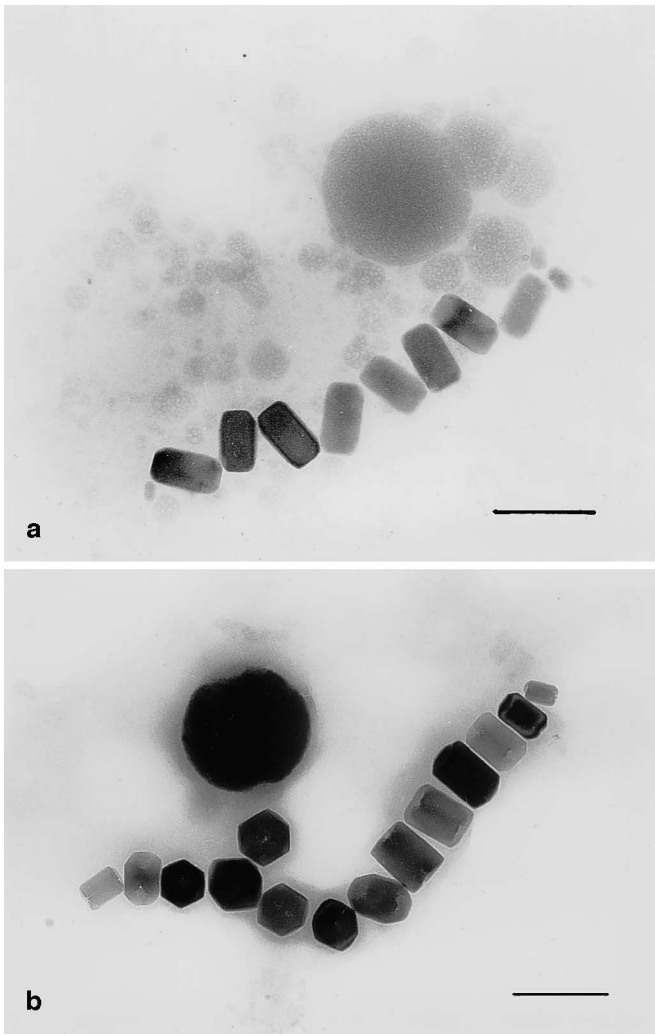

Fig. 9 a, b Strongly deformed configurations of magnetosome chains due to shrinkage of air-dried magnetic vibroid cells. Scale bars represent 0.2 microns. **a** Zig-zag-configuration. **b** Side-by-side-configuration

4 Discussion

Whatever it is composed of, the elastic material filling the gaps between the magnetosomes and preventing them from completely sticking together has a considerable effect on the structure of magnetosome chains by imparting flexibility to them. To prove this statement, we first assume that the modulus of elasticity of the gap filling is so large that the substance can be considered as incompressible. In this case, magnetostatic forces alone counteract an external force. The pecularity of these forces is that any change of configuration – no matter whether caused by tilting or by moving the particles away from each other – immediately gives rise to a strong response of the magnetostatic attraction (Eq. (23)). The corresponding stabilizing magnetostatic pressure is approximately M_{s}^2, indicating that a finite external force $T \geq T_{\text{crit}}$ needs to be applied so as to bring about any change of configuration. After the response of the magnetic forces is overweighted, they cannot prevent a further disruption of the chain and the results of such a strong external force may be strongly deformed (Fig. 9 a) or even completely demolished configurations (Fig. 9 b).

On the other hand, if the linear elastic properties of the gap filling are regarded, the response to a load is quadratic in tilting angle thereby giving rise to a finite flexural rigidity and enabling the chains to adapt to geometrical restrictions. However, as was stated above, elasticity may play a major role in the arrangement of bent configurations as long as the bending angle is relatively small, i.e. as long as an external force only slightly compresses the chain. Such a scenario is very plausible in a living bacterium if the chain is a little too long to fit the available space. In contrast, strong external forces, which will occur in air-dried cells due to shrinkage of the whole cell body, are most likely the cause for kinked chains or even strongly deformed configurations (Fig. 9).

Even in freeze-dried cells, in which the chains are not subject to large external forces, the loss of water can influence the elastic properties of the bonds between magnetosomes.

5 Conclusions

We calculated the stability of magnetosome chains for different scenarios by computing threshold values of external forces leading to bent or kinked chains. An important result is that long chains can be bent more easily than short chains (Eq. (19)), since the leverage of external forces is more effective on long chains. Additionally, smoothly bent chains reflect the elastic properties of the organic substance in the gaps. In contrast, sharp kinks can only be generated by magnetic interactions between the magnetosomes under strong external forces. This is in good accord with our TEM-investigations on freeze-dried cells which never revealed signs of strong deformations, whereas TEM-pictures of air-dried cells, which usually undergo considerably shrinking, often showed the phenomenon of kinking of the magnetosome chains.

Acknowledgements We thank H.-C. Bartscherer of the Institute of Physics, University München-Weihenstephan for the use of transmission electron microscopes (Zeiss EM 10, Philips CM 10 with tilting holder) and laboratory equipment. We also would like to thank Richard Frankel for valuable discussions. We acknowledge the helpful comments of two anonymous reviewers. This investigation was supported by grants Pe173/9-2&3 from the Deutsche Forschungsgemeinschaft (DFG). A research scholarship from the DFG enabled Valeri Shcherbakov's stay at the Institut für Geophysik in München.

References

Blakemore RP (1975) Magnetotactic bacteria. Science 190: 377–379

Butler RF, Banerjee SK (1975) Theoretical single-domain grain size range in magnetite and titanomagnetite. J Geophys Res 80: 4049–4058

von Dobeneck T, Petersen N, Vali H (1987) Bakterielle Magnetofossilien. Geowiss Zeit 1: 27–35

Duwe HP, Käs J, Sackmann E (1990) Bending elasticity and thermal excitations of lipid bilayer vesicles: modulation by solutes. Physica A 163: 410–428

Fabian K, Kirchner A, Williams W, Heider F, Leibl T, Hubert A (1996) Three-dimensional micromagnetic calculations for magnetite using FFT. Geophys J Int 124: 89–104

Frankel R, Blakemore B (1980) Navigational compass in magnetic bacteria. J Magn Magn Mater 15–18: 1562–1564

Gorby YA, Beveridge TJ, Blakemore RP (1988) Characterization of the bacterial magnetsome membrane. J Bacteriol 170: 834–841

Landau LD, Lifshits EM (1970) Lehrbuch der theoretischen Physik, Band 5 (Elastizitätstheorie), 3rd edn. Akademie-Verlag, Berlin

Kirschvink JL (1982) Paleomagnetic evidence for fossil biogenic magnetite in western Crete. Earth Planet Sci Lett 59: 388–392

Mutz M, Helfrich W (1990) Bending rigidities of some biological model membranes as obtained from the Fourier analysis of contour sections. J Phys France 51: 991–1001

Rhodes P, Rowlands G (1954) Demagnetising energies of uniformly magnetized rectangular blocks. Proc Leeds Philos Lit Soc Sci Sect 6: 191–210

Timoshenko SP, Gere JM (1961) Theory of Elastic Stability. Engineering Societies Monographs. MacGraw-Hill, New York

Appendix

The Rhodes-and-Rowlands formula for nonparallel surfaces

The magnetostatic energy of two parallel surfaces A and B, square in shape and of edge length a, each of which carries a homogeneous magnetic charge $M_s\sigma$ with $\sigma_A=-\sigma_B$ and which are separated by a distance $c=qa$, is given by

$$W_{ms}(A,B) = -M_s^2\,\sigma^2 \int_0^a dx \int_0^a dx' \int_0^a dy \int_0^a dy' \cdot \frac{1}{\sqrt{(x-x')^2+(y-y')^2+c^2}}, \tag{33}$$

(Rhodes and Rowlands 1954) where x, y and x', y' are the coordinates of square A and B, respectively. Evaluation of the two innermost integrals and subsequent substitution of $x-x'\to\xi$ leads to

$$W_{ms}(A,B) = 2\sigma^2 M_s^2 a^3 \int_0^1 dx \int_{x-1}^{x} d\xi \cdot [\sqrt{1+q^2+\xi^2} - \sqrt{q^2+\xi^2} + \log(-1+\sqrt{q^2+\xi^2}) - \log(\sqrt{1+q^2+\xi^2})]. \tag{34}$$

This kernel is the potential of two parallel lines of length 1 in y-direction lying a distance $z=q$ and $x=1$ apart from each other. To evaluate the potential of two squares which are inclined to each other by an angle θ, a parametric representation of the inclined surface A is required. According to Fig. 4b,

$$x \to x\cos\theta \quad \text{and} \quad q \to q + (x-0.5)\sin\theta \tag{35}$$

are the appropriate substitutions to be applied after the third integration. The fourth intergration over the range $x=[0, 1]$ has to be carried out numerically. The so obtained expression for $W_{ms}(A, B)$ (q, θ) is a generalized Rhodes-and-Rowlands formula that also accounts for inclined surfaces.

For the model showed in Fig. 4c, the substitutions are given by

$$x \to x\cos\theta \quad \text{and} \quad q \to q + x\sin\theta\,. \tag{36}$$